Tailoring the performance of nanocellulose-based multilayer-barrier paperboard using biodegradable-thermoplastics, pigments, and plasticizers

Koppolu, Rajesh; Johanna, Lahti; Abitbol, Tiffany; Aulin, Christian; Kuusipalo, Jurkka; Toivakka, Martti

Published in:
Cellulose

DOI:
10.1007/s10570-023-05281-x

Published: 01/07/2023

Document Version
Final published version

Document License
CC BY

Cellulose (2023) 30:6945–6958
https://doi.org/10.1007/s10570-023-05281-x

ORIGINAL RESEARCH

Tailoring the performance of nanocellulose-based multilayer-barrier paperboard using biodegradable-thermoplastics, pigments, and plasticizers

Rajesh Koppolu · Johanna Lahti · Tiffany Abitbol · Christian Aulin · Jurkka Kuusipalo · Martti Toivakka

Received: 12 February 2023 / Accepted: 21 May 2023 / Published online: 11 June 2023

Abstract In this work a multilayer barrier paperboard was produced in a roll-to-roll process by slot-die coating of nanocellulose (microfibrillated cellulose or carboxymethylated cellulose nanofibrils) followed by extrusion coating of biodegradable thermoplastics (polylactic acid, polybutylene adipate terephthalate and polybutylene succinate). Hyperplaty kaolin pigments were blended in different ratios into nanocellulose to tailor the barrier properties of the multilayer structure and to study their influence on adhesion to the thermoplastic top layer. Influence of a plasticizer (glycerol) on flexibility and barrier performance of the multilayer structure was also examined. Water vapor permeance for the multilayer paperboard was below that of control single-layer thermoplastic materials, and oxygen permeance of the coated structure was similar or lower than that of pure nanocellulose films. Glycerol as a plasticizer further lowered the oxygen permeance and kaolin addition improved the adhesion at the nanocellulose/thermoplastic interface. The results provide insight into the role played by nanocelluloses, thermoplastics, pigments, and plasticizers on the barrier properties when these elements are processed together into multilayer structures, and paves the way for industrial production of sustainable packaging.

R. Koppolu (✉) · M. Toivakka
Laboratory of Natural Materials Technology, Åbo Akademi University, 20500 Turku, Finland
e-mail: rajesh.koppolu@vtt.fi

M. Toivakka
e-mail: martti.toivakka@abo.fi

R. Koppolu · J. Lahti
Biomaterial Processing and Products, VTT Technical Research Center of Finland Ltd., 02150 Espoo, Finland
e-mail: johanna.lahti@vtt.fi

J. Lahti · J. Kuusipalo
Paper Converting and Packaging, Tampere University, 33100 Tampere, Finland
e-mail: johanna.lahti@vtt.fi

J. Kuusipalo
e-mail: jurkka.kuusipalo@tuni.fi

T. Abitbol · C. Aulin
RISE Research Institutes of Sweden, 11428 Stockholm, Sweden
e-mail: tiffany.abitbol@epfl.ch

C. Aulin
e-mail: christian.aulin@holmen.com

T. Abitbol
Materials Science and Engineering, EPFL - École Polytechnique Fédérale de Lausanne, 1015 Lausanne, Switzerland

C. Aulin
Holmen Iggesund, 11451 Stockholm, Sweden

Keywords Nanocellulose · Barrier · Packaging · Multilayer · Biodegradable · Roll-to-roll

Introduction

The global packaging market in 2021 was estimated to be approximately 1 trillion USD, and food packaging makes up about 30–35 % of the total packaging market (Future Market Insights 2021). Paper/paperboard, plastics, glass, wood, and metal are the most common materials used for food packaging, with paper/paperboard and plastics taking the largest share (Torres-Giner et al. 2021). Most often, food packaging is a multilayer structure comprising of paper/paperboard (for stiffness and rigidity) and one or several layers of plastics as functional layers for sealability and barrier properties against, e.g., water vapor, oxygen, grease, and mineral oils (Kaiser et al. 2017; Bauer et al. 2021). For demanding applications requiring long shelf-life and high oxygen-gas barrier, a metallized plastic layer is also used (Morris 2017a). While it is easier to recover and recycle mono-component packaging, it is very challenging to recycle the multilayer structures due to difficulty in separating the packaging into individual layers (Ragaert et al. 2017). In addition, the plastics used in multilayer packaging are often fossil-fuel based and are not biodegradable [for example, low/high density polyethylene (L/HDPE), polyethylene terephthalate (PET), polystyrene (PS), polypropylene (PP), polyvinyl chloride (PVC), ethylene-vinyl acetate (EVA), ethylene-vinyl alcohol (EVOH), and polyvinylidene chloride (PVDC)] (Morris 2017b). Therefore, most of the multilayer packaging ends up in landfills or is incinerated, which puts a considerable strain on natural resources and energy use (Kaiser et al. 2017; Stark and Matuana 2021).

Many countries around the world are introducing policy changes that are aimed at restricting the use of fossil-fuel-based plastics and encouraging the use of bio-based and biodegradable alternatives for packaging applications (Haider et al. 2019). European Union(EU)'s circular economy action plan adopted in March 2020 (Commission and for Communication 2020) and Ellen MacArthur Foundation's New Plastics Economy Global Commitment launched in October 2018 (in collaboration with the United Nations Environment Program) (Foundation 2021) are examples of such initiatives. In addition, recent years have seen a shift in consumer preferences towards more bio-based products (Gaffey et al. 2021; Delioglamnis et al. 2018). All this has resulted in an increased interest from academia and industry towards finding sustainable barrier packaging solutions (Tyagi et al. 2021).

Nanocellulose (or cellulose nano fibers—CNFs) is a cellulose-based natural polymer that has gained considerable interest in recent years due to its outstanding barrier against oxygen, grease, and mineral oils (Abitbol et al. 2016; Thomas et al. 2018; Ahankari et al. 2021; Wang et al. 2018). Nanocellulose is both bio-based and biodegradable, and therefore, nanocellulose-based coatings and films are being considered as a potential replacement to non-biodegradable plastics and metallic aluminum layers in food packaging applications (Tyagi et al. 2021; Cherian et al. 2022). Several companies have already started producing nanocellulose at pilot or commercial-scale to be used primarily for barrier applications (FutureMarkets 2021), with many research groups including the authors of this work demonstrating roll-to-roll (R2R) coating of nanocellulose on paper/paperboard using slot-die (Kumar et al. 2016; Koppolu et al. 2018, 2019, 2022; Jung et al. 2022), gravure (Chowdhury et al. 2018), spray coating (Shanmugam 2022; Satam et al. 2018; Beneventi et al. 2014, 2015), and wet lamination (Guerin et al. 2020) methods.

Despite their barrier against oxygen and greases, nanocellulose-based coatings suffer from poor water vapor barrier due to hygroscopic nature of cellulose (Spence et al. 2011). This issue can be addressed by having a moisture barrier coating on top of the nanocellulose layer to protect the latter from humidity (Koppolu et al. 2019; Tyagi et al. 2021; Cherian et al. 2022). This multilayer structure can be made sustainable by choosing a moisture-barrier coating material that is bio-based and biodegradable (Vartiainen et al. 2016). Several research articles have demonstrated such multilayer barrier structures by utilizing various biodegradable polymers such as guar gum (Dai et al. 2017), alginate (Zhao et al. 2020), alkyd resins (Aulin and Strö 2013), polyglycolic acid (Vilarinho et al. 2018), polyhydroxy alkanoates (PHAs) (Cherpinski et al. 2018), shellac (Hult et al. 2010), chitin (Satam et al. 2018), and polylactic acid (PLA) (Aulin et al. 2013; Koppolu et al. 2019).

Mineral pigments such as kaolins and talc are frequently employed as fillers in the polymer phase of water-based barrier dispersions (Martinez-Hermosilla et al. 2015; Zhu et al. 2019). This is because they increase the tortuosity of the permeant through the coating structure, thereby enhancing the barrier properties of the material (Bollström et al. 2013; Sun et al. 2007). Additionally, the use of mineral pigments is cost-effective since they can replace some of the more expensive polymers in the dispersion (Zhu et al. 2019). Several researchers have investigated the effect of blending different types of kaolinite or montmorillonite into nanocellulose and have reported improvements in barrier properties (Al-Gharrawi et al. 2022; Aulin et al. 2012; Alves et al. 2019). Plasticizers are also frequently employed in barrier coatings to enhance the flexibility of the barrier layer (Vieira et al. 2011; Lin and Krochta 2003). Commonly used plasticizers include polyethylene glycol, monosaccharides (glucose, fructose), glycerol, sorbitol, and polyvinyl alcohol (PVOH) (Sothornvit and Krochta 2005). The impact of plasticizer addition on the barrier properties of nanocellulose has also been investigated in the scientific literature (Herrera et al. 2017; Fernandez-Santos et al. 2021).

In our previous work (Koppolu et al. 2019), we demonstrated a multilayer barrier paperboard produced by slot-die coating of microfibrillated cellulose (MFC) or cellulose nanocrystals (CNCs), followed by extrusion coating of PLA. The resulting paperboard showed promising barrier against oxygen, grease, mineral oil, and water vapor. However, a few challenges were identified such as, poor adhesion at nanocellulose-extrusion polymer interface and, poor flexibility of CNC-coated paperboard due to brittle nature of CNC coatings (especially at higher humidity). The current work aims to address the above-mentioned issues, and to further understand and optimize the performance of nanocellulose-based multilayer barrier paperboard. CNF produced via carboxymethylation pretreatment (Naderi et al. 2015; Wågberg et al. 2008) was used in place of CNCs, and polymers with higher biodegradability such as, polybutylene adipate terephthalate (PBAT) and polybutylene succinate (PBS) were used for extrusion coating. Hyperplaty kaolin pigments were blended in different ratios into nanocellulose to tailor the barrier properties of the multilayer structure and to study their influence on adhesion with thermoplastic top layer. Influence of plasticizers on flexibility and barrier performance of roll-to-roll coated nanocellulose layer was also examined.

Materials and methods

Materials

MFC was supplied as a 20% w/w cake by The Process Development Center of University of Maine (USA) and was diluted to 2.5% for R2R coating. Carboxymethylated-CNF was supplied as a 2% w/w suspension by RISE Research Institutes of Sweden (Sweden) and used without dilution. Brief descriptions of the production processes for both nanocellulose grades is given in the supporting information. Carboxymethyl cellulose (CMC, Finnfix® 4000 G, CP Kelco, Finland) was added as rheology modifier at 5% w/w (with respect to dry nanocellulose) to both the suspensions. The description of rheology measurements and influence of CMC addition on MFC and CNF suspensions' yield stress are given in the supporting information. A more detailed discussion on the role of rheology during continuous coating of nanocellulose can be found in Koppolu et al. (2022).

Hyperplaty kaolin (Barrisurf^{TM} HX, Imerys U.K) [aspect ratio 100:1] was blended into MFC to study the influence of pigment addition on barrier properties of nanocellulose-coated paperboard, and adhesion at nanocellulose/thermoplastic interface. MFC-kaolin composite films (thickness – 20 µm) with varying kaolin ratios (10, 20, 40, and 50%) were first prepared by casting 0.5% MFC-kaolin suspension in petri dishes and evaporated at 23 °C and 50% relative humidity (RH). Mineral-oil barrier test (Heptane vapor transmission rate—HVTR) for the composite films indicated a significant loss of barrier at kaolin addition levels higher than 20% by dry weight (see supporting information for description of the test procedure and HVTR of MFC-kaolin composite films). Therefore, 10 and 40% kaolin addition levels were chosen for R2R coatings to represent both ends of the barrier spectrum (see Table 1 for information on R2R coated trial points).

Three different plasticizers, viz., CMC (Finnfix® 4000 G, CP Kelco, Finland), polyvinyl alcohol—PVOH (Mowiol® 23-98, Kuraray, Finland), and glycerol (>99.5%, Sigma Aldrich, Finland)

Table 1 List of different nanocellulose and thermoplastic-based coatings produced in this work

Coating layer[a]	Coating method	Suspension solids content[b] (%)	Coating speed ($m.min^{-1}$)	Wet thickness[c,d] (µm)	Dry thickness[e] (µm)	Coated length (m)
MFC	Slot-die	2.5	2.5	400	8 ± 2 ($\approx 12\ g.m^{-2}$)	37
90%MFC+ 10%Kaolin	Slot-die	2.8	2.5	400	10 ± 2 ($\approx 16\ g.m^{-2}$)	34
60%MFC+ 40%Kaolin	Slot-die	4.0	3	400	8 ± 1 ($\approx 15\ g.m^{-2}$)	37
CNF	Slot-die	2	6	250×2	5 ± 1 ($\approx 7\ g.m^{-2}$)	33
CNF+2% Glycerol	Slot-die	2	6	250×2	5 ± 1 ($\approx 8\ g.m^{-2}$)	22
CNF+10% Glycerol	Slot-die	2	6	250×2	4 ± 1 ($\approx 7\ g.m^{-2}$)	10
LDPE	Hot-melt extrusion	–	70	–	18 ± 1 ($\approx 17\ g.m^{-2}$)	51 + (9)[f]
ecovio®	Hot-melt extrusion	–	70	–	28 ± 2 ($\approx 38\ g.m^{-2}$)	51
PBS	Hot-melt extrusion	–	70	–	17 ± 1 ($\approx 22\ g.m^{-2}$)	51

[a]MFC and CNF have 5% CMC added with respect to dry nanocellulose; MFC and Kaolin are blended in the ratios mentioned; Glycerol is added with respect to dry CNF

[b]For all MFC suspensions, MFC to water ratio was kept constant at 2.4% (see supporting information for influence of MFC to water ratio on viscosity of MFC-kaolin suspensions

[c]Wet thickness is the set value between slot-die's top lip and paper substrate

[d]CNF-layers were double coated

[e]Dry thickness is measured value from SEM cross-sections. Coat weights are calculated assuming densities of 1.55, 2.65, 0.94, 1.36, 1.26 $g.cc^{-1}$ for nanocellulose, kaolin, LDPE, ecovio®, and PBS respectively

[f]Few meters of MFC containing coatings were coated with LDPE on the backside of paperboard (in addition to top side coating)

were added to CNF to study their influence on flexibility and barrier performance of the CNF-coated layer. CNF films (thickness – 20 µm) with varying plasticizer ratios (2, 5, and 10% w/w added with respect to dry CNF) were first prepared by casting 0.5% CNF-plasticizer suspensions in petri dishes and evaporated at 23 °C and 50% RH. The mechanical properties of these films, evaluated using a Universal Testing Machine 8872 (Instron, Germany), showed that glycerol containing CNF films had the highest elongation at break compared to CMC and PVOH as plasticizers (detailed information on elongation at break for CNF films is given in supporting information). Therefore, 2 and 10% w/w glycerol was added to CNF for R2R coatings (see Table 1 for information on R2R coated trial points).

A pigment-coated paperboard (Trayforma™ Special, Stora Enso, Finland, $205 \pm 1.5\ g.m^{-2}$ and 270 ± 1.5 µm), referred to as "baseboard", was used as a base substrate for all of the coatings described in this work. The baseboard was pre-coated with a 0.3% w/w cationic starch (Raisamyl® 135, Chemigate, Finland) solution to improve adhesion at the nanocellulose/paperboard interface (Koppolu et al. 2018). The nanocellulose-coated paperboard was further coated with three different types of thermoplastics viz., LDPE (Borealis), ecovio® [PBAT, PLA blend] (BASF), and PBS (BioPBS™, PTT MCC Biochem) to provide moisture barrier. LDPE was used as a reference, while ecovio and PBS were chosen as biodegradable thermoplastics (Siegenthaler et al. 2011; Aliotta et al. 2022; Zhao et al. 2005).

Coating process

The cationic starch primer-coating was first applied onto the baseboard using a laboratory-scale roll-to-roll reverse gravure coater (Rotary Koater, RK Print-Coat Instruments, U.K) [gravure roll: 70 lpi × 127 µm with a surface volume of 78.5 $cm^3.m^{-2}$; dry coat weight < 1 $g.m^{-2}$]. MFC and CNF suspensions were then coated on top of the starch-coated baseboard using the same R2R coater fitted with a slot-die applicator. A detailed description of the working principles of slot-die coating of nanocellulose suspensions is provided in our previous work (Koppolu et al. 2018, 2019, 2022), and is briefly discussed in the supporting information of the current work. Table 1 lists the different nanocellulose coatings done in this work along with their respective wet thicknesses (set value), line speeds, and dry-coating thicknesses (measured value). All nanocellulose-coated paperboards were then calendered at 100 $kN.m^{-1}$ and 60 °C using a laboratory-scale soft nip calender (DT Paper Science, Finland).

The nanocellulose-coated paperboards were finally coated with the above-mentioned thermoplastics (LDPE, ecovio®, and PBS) using a pilot-scale extrusion coater at Tampere University (Finland). Prior to extrusion coating, all the samples were corona treated (inline) to improve the adhesion between nanocellulose and thermoplastic layers. Coating speed was set at 70 $m.min^{-1}$ and the coating thickness for each polymer was chosen according to the supplier's recommendation (Table 1).

Characterization of coated samples

Transmission electron microscope (TEM) images of the nanocellulose suspensions were obtained using JEOL JEM-1400 Plus (JEOL, Japan) at 80 kV acceleration voltage. All the coated samples were conditioned at 23 °C and 50 % RH for at least 24 h before characterization and unless specifically stated, all measurements were done under these conditions. Cross-section images for the coated samples were obtained using a field-emission scanning electron microscope (FE-SEM) [LEO Gemini 1530, Carl Zeiss, Germany]. Coating thicknesses for each layer was measured from cross-section images and the corresponding coat weights were calculated using respective layer's density (assuming a densely packed structure for each layer) [see Table 1].

Adhesion at the nanocellulose/thermoplastic interface was determined by measuring the force required to peel off a tape (TZe-C51, Brother, UK) attached to the paperboard's surface using an IMASS SP-2000 (USA) peel tester. One edge of the tape was attached to the surface of the substrate, while the opposite edge was clamped to a 50 *N* load cell. The tape was pulled at an angle of 180° over a length of 26 mm at a speed of 5 $mm.s^{-1}$, and the force required to peel the tape was measured as a function of peeling distance. There is an initial force peak as the coated layer fractures at the weaker interface, after which the force plateaus to a lower value as the fractured-layer is peeled off. The average peak force from five parallel measurements is reported. An example of the peel force versus peeled length is given in supporting information.

Attenuated total reflectance—Fourier transform infrared spectroscopy (ATR-FTIR) was used to determine the orientation of kaolin-pigment particles in both MFC-kaolin composite films and R2R coated samples according to the method described by Elton et al. (1999) and Bollström et al. (2013). Nicolet™ iS50 FTIR Spectrometer (Thermo Scientific, USA) with a diamond KRS5 ATR crystal and an incidence angle of 45° was used for ATR-FTIR measurements. The particle alignment factor ($k = I_{3695}/I_{3620}$) of kaolin pigments on the surfaces of the films and coated samples was determined by comparing the –OH absorption peaks of kaolin above 3500 cm^{-1}. The peak at 3695 cm^{-1} (I_{3695}) shows the –OH group that is perpendicular to kaolin surface; and the peak at 3620 cm^{-1} (I_{3620}) shows the –OH group that is at a shallow angle to the kaolin's surface. A low value of k indicates higher alignment to the surface and vice-versa.

Water vapor permeance (WVP) was determined according to ASTM E96/E96M-05 at two different conditions, 23 °C/50% RH and 38 °C/90% RH, and an average from three parallel measurements is reported as $gm^{-2}\,day^{-1}\,kPa^{-1}$. Oxygen permeance (OP) was measured according to ASTM F1927-07 (coulometric method) [Ox-Tran 2/21 MH/SS, Mocon, U.S.A] or ASTM F3136-15 (dynamic accumulation method) [OpTech-O2 Model P, Mocon, U.S.A] at 23 °C/50% RH. A few LDPE-coated samples were also measured at 25 °C/75% RH and 38 °C/90% RH. F3136 is a relatively fast method to determine oxygen barrier for

medium to low barrier materials, and was first used to screen out low oxygen-barrier samples. F1927 is more sensitive to defects and is used for high oxygen-barrier materials. OP from two parallel measurements is reported as $cc.m^{-2}.day^{-1}.bar^{-1}$. Grease barrier was evaluated according to ASTM F119-82 using olive oil at 40 °C, and the average value from three parallel measurements is reported in hours (in the interest of time, the test was stopped after 500 h). HVTR (mineral oil barrier) for the coated samples was determined according to the method suggested by Miettinen et al. (2015), and the average value from three parallel measurements is reported as $g.m^{-2}.day^{-1}$. Detailed test procedures for grease and mineral oil barrier is given in the supporting information.

Results and discussion

Nanocellulose structure

TEM images show coarser fibrils for MFC and a finer structure for CNF (Fig. 1), mainly due to the latter's chemical pre-treatment and fiber delamination process (high-pressure homogenization). Although MFC is coarser, it has enough nano material to form tightly packed structures, and is expected to give similar barrier properties as CNF. However, CNF could achieve the required barrier properties at a lower coat weight. On the other hand, CNF has a higher viscosity (compared to MFC) due its finer structure and higher charge (from carboxymethylation pre-treatment), and therefore the solids content used for coating is kept lower than that of MFC. Ultimately, the choice of nanocellulose depends on the end user's requirements viz., cost, barrier performance, application method, drying capacity, and make-up of the barrier structure.

Coating structure

Figure 2 shows SEM cross-section images for the multilayer-coated paperboards produced in this work, where, both nanocellulose and thermoplastic layers are clearly visible. It can be noticed from Fig. 2d–f, that the adhesion at nanocellulose/thermoplastic (ecovio® and PBS) interface is poor and there is clear delamination between the layers. The delamination is more pronounced for CNF-coated paperboard. Although Fig. 2a–c, do not show any delamination, the adhesion between nanocellulose and thermoplastic (LDPE) is still low (see Fig. 3a), and may cause serious problems during converting operations, including creasing, folding, and sealing. This poor adhesion occurs despite corona pre-treatment, and could be attributed to the incompatibility between polar and non-polar groups of nanocellulose and thermoplastics, respectively.

Adhesion

Insufficient adhesion between dissimilar layers is a common problem in multilayer packaging structures. The adhesion can be improved either by using tie-layers (functionalized polyolefins, such as maleic anhydride-modified Linear-LDPE) or by promoting mechanical interlocking by, e.g., increasing the surface roughness (Morris 2017b). Figure 2g and h show SEM cross-sections of multilayer-coatings containing PBS and kaolin-blended MFC (SEM cross-sections of LDPE and ecovio® coatings on kaolin-blended MFC are given in supporting information). Compared to Fig. 2e, an improvement in adhesion at the MFC/PBS interface is clearly visible. A tape test was done to quantify adhesion at the thermoplastic/MFC interface by measuring the peak peel force required to fracture the interface (Fig. 3a). Peel force reduced

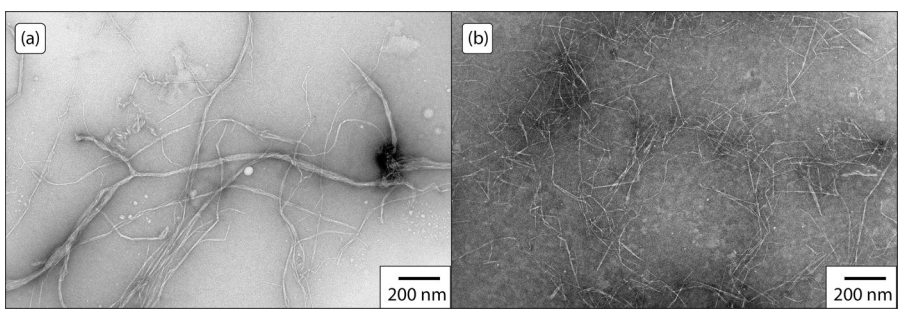

Fig. 1 TEM images of **a** MFC, **b** CNF

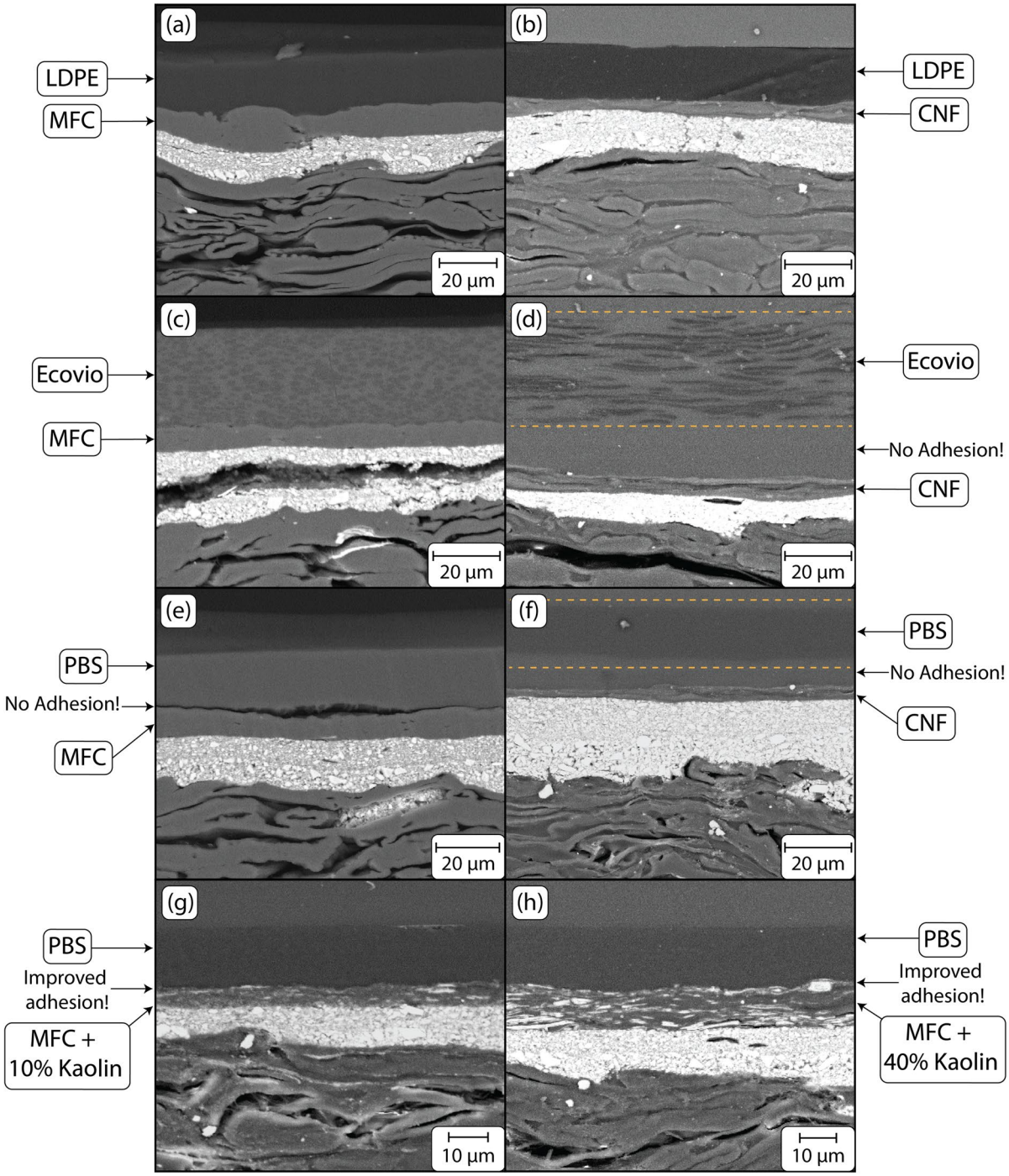

Fig. 2 SEM cross-sections for the multilayer-coated samples: **a** MFC + LDPE; **b** CNF + LDPE; **c** MFC + ecovio®; **d** CNF + ecovio® [ecovio® layer is completely separated—shown between the dashed lines]; **e** MFC + PBS; **f** CNF + PBS [PBS layer is completely separated—shown between the dashed lines]; **g** MFC+10%kaolin + PBS; **h** MFC+40%kaolin + PBS. *Note* Base layer for all coatings is pigment coated paperboard with cationic starch pre-coating; starch layer not visible in the SEM cross-sections due to its low coat weight (<1 $g.m^{-2}$)

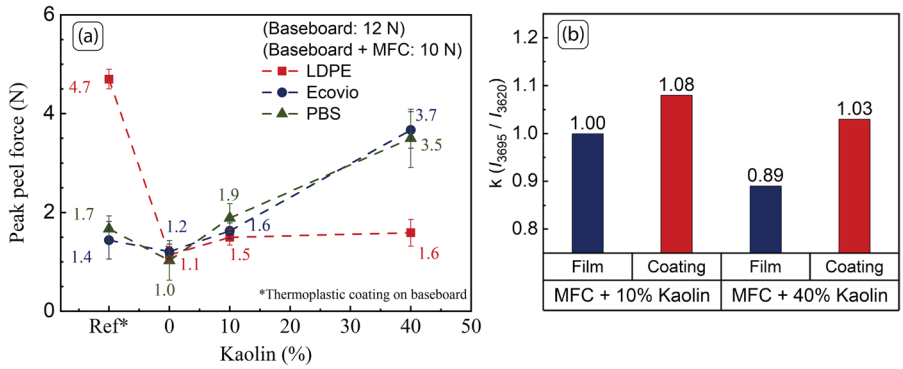

Fig. 3 **a** Peak peel force for multilayer coatings as a function of kaolin addition level; **b** Kaolin alignment factor ($k = I_{3695}/I_{3620}$) for petri dish films and R2R coated samples

significantly when thermoplastics were coated on pure MFC, compared to the corresponding single-layer thermoplastic coating on paperboard. As the kaolin content in MFC increased, the peel force and therefore, adhesion between MFC and thermoplastic layers improved. For Ecovio and PBS, the peak peel force increased by 2-fold when the kaolin content reached 40%, compared to the coatings on pure MFC.

Figure 3b shows the kaolin alignment factor (k) determined from ATR-FTIR measurements for MFC-kaolin composite petri-dish films and R2R coated samples. A lower value of 'k' indicates higher particle alignment with respect to the surface plane (Elton et al. 1999; Bollström et al. 2013). It can be seen from the figure that the kaolin pigments have higher alignment in petri-dish films compared to the R2R coated samples. During petri-dish film preparation, the suspension's solids content is initially very low (ca. 0.5%), which allows the platy-pigment particles to align more easily as there is less crowding of MFC around the pigment particles. Also, the slow drying conditions during petri-dish film preparation provides more time for the platy particles to orient along the surface due to the surface tension forces in the contracting layer. In contrast, during R2R coating, the solids content of the MFC suspensions is much higher (ca. 3–4%) and the drying process is faster, which makes it harder for the kaolin pigments to align in the direction of the flow (or along the surface). This increases the surface roughness of the coated MFC-layer (see supporting information for SEM surface images of MFC-kaolin coated paperboard), which then leads to higher mechanical interlocking of the thermoplastic layer and therefore an improved adhesion. It is to be noted that blending pigments into MFC may disturb the closely packed microstructure of the nanocellulose-layer and therefore can result in reduced barrier performance as will be discussed in the next subsections.

Oxygen barrier

Petri dish films versus roll-to-roll coated samples

Nanocellulose films prepared using laboratory-scale batch processes exhibit excellent barrier against oxygen, and are comparable to the values obtained by PVDC, EVOH, and metallized PET, which are commonly used oxygen barrier materials in packaging applications (Ahankari et al. 2021; Lindström and Österberg 2020; An et al. 2018). Figure 4a shows the oxygen permeance values for MFC and CNF petri-dish films and R2R coated samples at 23 °C/50 % RH. OP of the petri-dish films is normalized to the same thickness as that of the R2R coated nanocellulose layer for better comparison. The oxygen barrier of the R2R coated nanocellulose is poor, with an OP (ca. 5000 $cc.m^{-2}.day^{-1}.bar^{-1}$) that is approximately 500 times higher than that of pure petri dish films (ca. 10 $cc.m^{-2}.day^{-1}.bar^{-1}$). During R2R coating, the wet nanocellulose layer is dried very quickly (less than 2 min.) under harsh conditions where temperatures in the dryers can reach 200 °C. This leads to cracks/defects in the dried nanocellulose layer and therefore, results in a poor oxygen barrier. In contrast, the slow drying and mild self-assembly conditions used to make petri dish films result in a uniform and dense nanocellulose network required for oxygen barrier.

Thermoplastics such as LDPE, PLA, PBAT, and PBS show poor oxygen barrier as oxygen molecules easily diffuse through these materials (Wu et al.

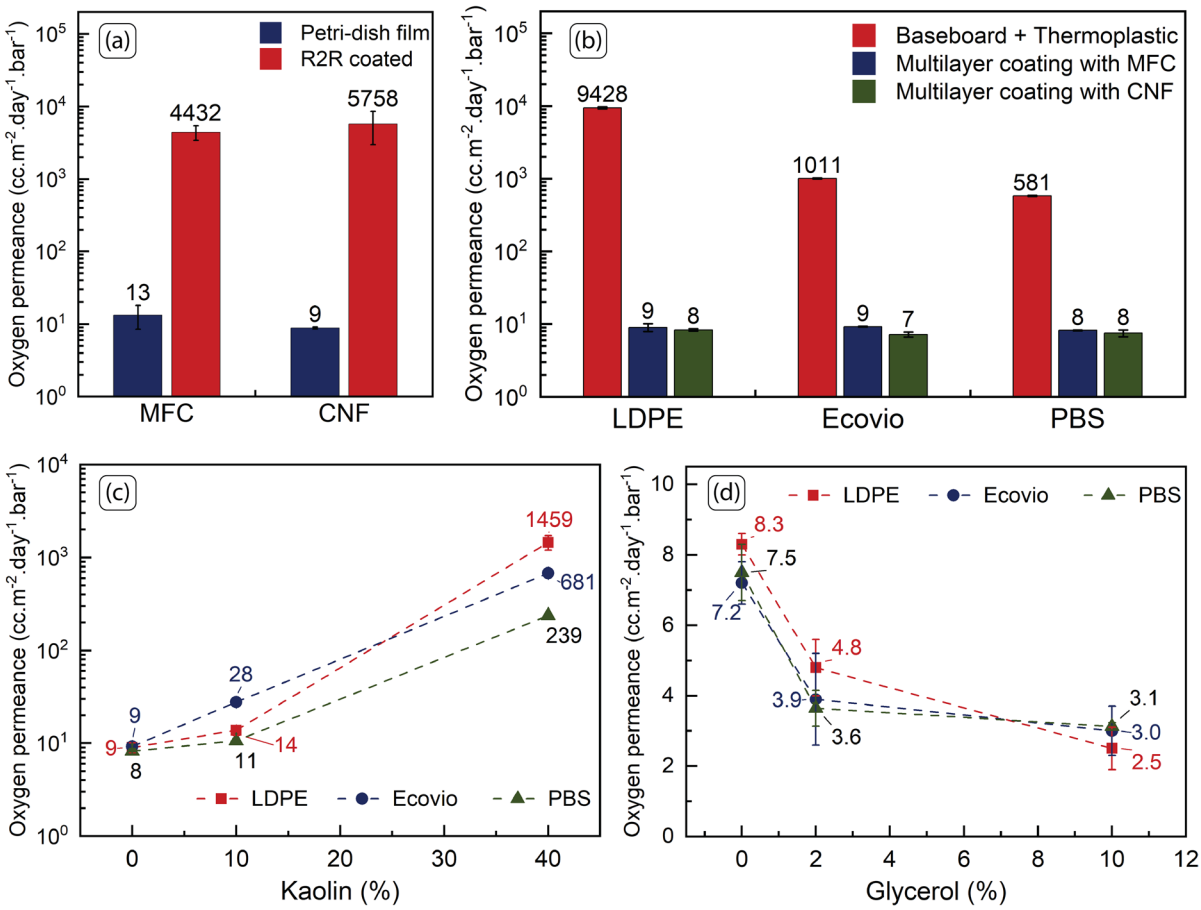

Fig. 4 Oxygen permeance at 23 °C/50% RH for, **a** Nanocellulose films and R2R coatings of similar thicknesses; **b** Multilayer coated paperboards and corresponding reference single layer thermoplastic coatings; **c** influence of blending Kaolin into MFC; **d** influence of glycerol addition to CNF

2021) (Fig. 4b). Interestingly, extrusion coating of thermoplastics onto nanocellulose-coated paperboard, restores the latter's OP to the same level as that of their corresponding pure petri-dish films (Fig. 4b). These findings are consistent with the observations made in our previous work (Koppolu et al. 2019). An explanation for the improved OP of multilayer paperboard might be that the extrusion-coated polymer fills up/seals any cracks or pinholes in the nanocellulose layer, and since the relative area of these pinholes or cracks is very small, just sealing them can be sufficient to restore the oxygen barrier. Nevertheless, it is promising that R2R produced multilayer paperboard containing nanocellulose and thermoplastics can achieve similar OP values as that of pure films of equivalent thickness.

Pigment and plasticizer addition

As discussed in the above "Adhesion" section, adding pigments into nanocellulose helps improve the adhesion at the nanocellulose/thermoplastic interface. However, this might negatively affect the barrier properties of nanocellulose layer as the pigment particles may interfere with the closely packed microstructure of nanocellulose. Figure 4c shows the OP of MFC-containing multilayer paperboard with varying kaolin ratios. As expected, OP increases with higher kaolin levels, and at 40% kaolin, the oxygen permeance is 1–2 orders of magnitude higher than that of a pure MFC layer. However, at a low kaolin ratio of 10%, the OP is quite similar to that of pure MFC coating and therefore may be suitable for applications

with medium oxygen barrier requirements, as long as sufficient adhesion with the thermoplastic layer is maintained. Therefore, by optimizing the pigment addition level, it is possible to tailor the multilayer structure to achieve the desired oxygen barrier and inter-layer adhesion, while using less (and more expensive) nanocellulose. For demanding oxygen barrier applications, one can also coat a separate thin kaolin (or pigment) layer on top of nanocellulose to aid in the adhesion with the thermoplastic top layer.

Plasticizers such as glycerol improve the flexibility of nanocellulose films significantly. For example, 2 and 10% glycerol addition increases the strain at break of 20 µm thick CNF-based films from 2.1% to 5.4 and 14.8%, respectively (see supporting information for more details on the influence of CMC, PVOH, and glycerol plasticizers on the mechanical properties of CNF films). The increased flexibility reduces the probability of crack formation during R2R coating. It is evident from Fig. 4d that with the addition of glycerol, OP of CNF-containing multilayer paperboard further decreases from ca. 7.5 cc.m^{-2}.day^{-1}.bar^{-1} to a lowest value of 2.5 cc.m^{-2}.day^{-1}.bar^{-1} for 10% glycerol addition at 23 °C/50% RH. Surprisingly, this OP value is similar to that of pure CNF film of equivalent thickness at 0% RH! (The OP of a 5 µm CNF film at 0% RH is 3.1 cc.m^{-2}.day^{-1}.bar^{-1}). Barrier packaging paperboard is usually formed into different shapes by creasing or folding according to the end use, and plasticizers could play a vital role in preserving the barrier properties during the converting operations. Therefore, future work should clarify the role of plasticizers on barrier properties after such converting processes.

Influence of moisture and temperature on oxygen barrier properties

Nanocellulose swells at high humidity and as a result, its dense microstructure loosens as the humidity increases. This lowers the barrier performance of nanocellulose coatings, and higher temperatures (high vapor pressure) accelerate it even more. Oxygen permeance of MFC+LDPE coated paperboard was further measured at two additional conditions, 25 °C/75% RH and 38 °C/90% RH (Fig. 5a). As the temperature and humidity increase, OP of the multilayer structure also increases. Although LDPE coating protects MFC from moisture, water vapor can still diffuse through the backside of the paperboard and swell the MFC layer. To counter this, an additional layer of LDPE was coated on the backside of the paperboard and the resulting OP values are shown in Fig. 5a. Backside LDPE coating reduced OP of the MFC containing multilayer paperboard at 38 °C/90% RH from 1305 to 411 cc.m^{-2}.day^{-1}.bar^{-1}, but it is still quite high for most applications. The reason for the high OP values may be that the water vapor is diffusing in through the paperboard's cross-section. The influence of humidity can potentially be further reduced by sandwiching the nanocellulose coating in-between two thermoplastic layers, thereby reducing the cross-sectional area that is exposed to the environment. However, this requires some optimization of the drying section and inter-layer adhesion, which we plan to address in a future work.

Water vapor barrier

Figure 5b shows the water vapor permeance at two different test conditions for single-layer nanocellulose and thermoplastic-coated paperboard. As expected, both MFC and CNF coated paperboards do not show

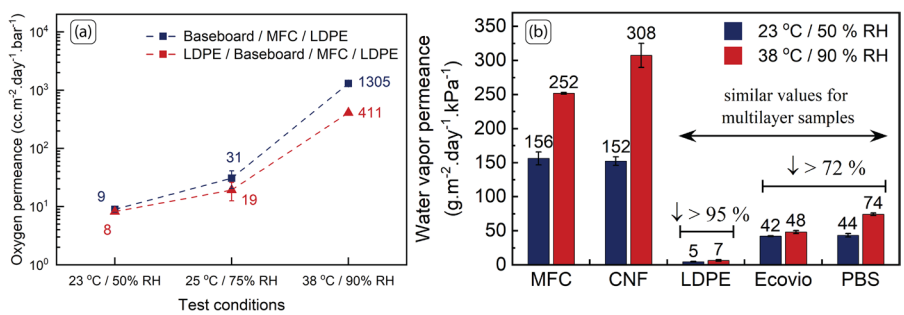

Fig. 5 **a** Oxygen permeance at different test conditions for MFC/LDPE and LDPE/MFC/LDPE multilayer coatings; **b** WVTR at different test conditions for single layer coatings on paperboard

any barrier against water vapor. Thermoplastics on the other hand, show a significant reduction in WVP with LDPE showing the highest reduction of over 95%, and ecovio® and PBS showing a reduction of > 72%. Most biodegradable thermoplastics are susceptible to hydrolysis (Rudnik 2013), especially at higher temperatures and humidities, and therefore show higher WVP than LDPE. Multilayer-coated paperboards show the same WVP as that of the corresponding top layer thermoplastic coating.

Grease and mineral-oil barrier

Figure 6a shows the grease barrier for the single-layer coated samples produced in this work. The starting point of the bar indicates failure of the first sample and the end indicates failure of the last sample. Similar to OP values, both MFC and CNF single-layer coatings show a wide variation in the grease barrier due to pinholes or cracks present in the dried coating structure. MFC and CNF-coated paperboards have grease barrier in the range of 90–270 and 50–450 h, respectively. Blending kaolin into MFC lowered the grease barrier, while glycerol addition showed less of an impact. Analogously to the oxygen barrier, when coated with a thermoplastic layer on top, the grease barrier improves, showing no failures during the test period of 500 h.

Both MFC and CNF-coated paperboards show excellent barrier against mineral oils, with no *n*-heptane vapors escaping through the structure during the test period. Ecovio® and PBS coated paperboards also show similar barrier against *n*-heptane. LDPE as such has poor mineral oil barrier with a HVTR value of ca. 640 $g.m^{-2}.day^{-1}$, but when coated on top of MFC shows zero HVTR. Figure 6b shows the HVTR of a single layer MFC coating and a multilayer with LDPE plotted as a function of kaolin content. At 10% kaolin ratio, the HVTR is still below the reliable detection limit and increases with higher kaolin ratios. This aligns with the observations made in the discussion of the grease and oxygen barrier performance, specifically that a small amount of pigment can be blended into nanocellulose without unduly compromising barrier properties.

Conclusion

Two different grades of nanocelluloses, MFC (pure mechanical defibrillation) and CNF (carboxymethylation pre-treatment followed by microfluidization) were roll-to-roll coated using a slot-die applicator on paperboard. To protect nanocellulose from moisture, thermoplastics such as LDPE (non-biodegradable reference), ecovio® (PLA, PBAT-based biodegradable polymer), and PBS (biodegradable polymer) were extrusion coated on top of the nanocellulose to obtain a multilayer structure. Blending pigments such as kaolin into MFC improves the adhesion at nanocellulose-thermoplastic interface. Water vapor barrier of the multilayer-coated samples remained below the control single-layer thermoplastic materials. Extrusion coating also helped plug any defects or pinholes in the nanocellulose layer, thereby improving the oxygen and grease barriers, with OP values similar to those of pure nanocellulose films of equivalent thicknesses. Kaolin addition to MFC increases the OP, but the ratio of kaolin could be controlled to tailor the oxygen barrier according to end use application. Plasticizers such as glycerol increase the flexibility of nanocellulose layer, thereby reducing the coating defects, and further bringing down the OP values. Having a moisture-barrier coating on the backside of

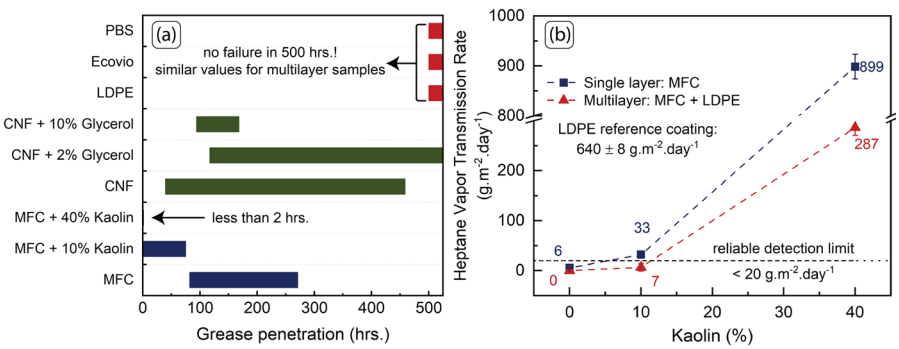

Fig. 6 **a** Grease barrier for single-layer R2R coated samples [starting of bar indicates failure of first sample and ending point indicates failure of last sample]; **b** HVTR versus kaolin addition level for single layer MFC and MFC+LDPE multilayer coated samples

the paperboard protects nanocellulose from moisture at high humidities, however, the oxygen permeance is likely still high due to moisture seeping in through the paperboard's cross-section. Sandwiching nanocellulose in-between two moisture barrier materials could potentially further protect nanocellulose from the effects of humidity.

This approach of processing nanocellulose and biodegradable thermoplastics together into a multilayer structure complements the shortcomings of each distinct component, enabling the production of a bio-based and biodegradable paperboard with excellent oxygen, water vapor, grease, and mineral oil barriers. Moreover, by controlling the type and amount of nanocelluloses, thermoplastics, pigments, plasticizers, and rheology modifiers, the barrier properties of the final multilayer structure can be tailored to suit specific end use applications.

Acknowledgments The authors thank the following persons and companies for their respective contributions. Prof. Douglas Bousfield, University of Maine for MFC. CP-Kelco for CMC. Imerys for Barrisurf HX. Chemigate for Cationic starch. Stora Enso for TrayForma™ paperboard. Luyao Wang for TEM. Diosángeles Soto Véliz for grease barrier characterization. Himal Ghimire for help with slot-die coatings.

Author contributions RK: experiment planning, execution, characterization, writing—original draft. JL: experiment planning, extrusion coating, oxygen barrier measurements, writing—review and editing. TA: experiment planning, adhesion measurements, writing—review and editing. CA: experiment planning, supervision, writing—review and editing. JK: experiment planning, supervision, writing—review and editing. MT: main supervisor, experiment planning, writing—review and editing.

Funding Open access funding provided by Åbo Akademi University (ABO). RK received funding from Åbo Akademi Graduate School of Chemical Engineering, Magnus Ehrnrooth foundation, Finnish Forest Products Engineers Association, and Walter Ahlström Foundation.

Data availability All the data and materials are available within this article.

Declarations

Conflict of interest The authors have no relevant financial or non-financial interests to disclose.

Ethics approval and consent to participate Not applicable.

Concent for publication All authors have approved this submission.

References

Abitbol T, Rivkin A, Cao Y et al. (2016) Nanocellulose, a tiny fiber with huge applications. Curr Opin Biotechnol 39:76–88. https://doi.org/10.1016/j.copbio.2016.01.002

Ahankari SS, Subhedar AR, Bhadauria SS et al. (2021) Nanocellulose in food packaging: a review. Carbohydr Polym 255(117):479. https://doi.org/10.1016/j.carbpol.2020.117479

Al-Gharrawi M, Ollier R, Wang J et al. (2022) The influence of barrier pigments in waterborne barrier coatings on cellulose nanofiber layers. J Coat Technol Res 19(1):3–14. https://doi.org/10.1007/s11998-021-00482-0

Aliotta L, Seggiani M, Lazzeri A et al. (2022) A brief review of poly (butylene succinate)(pbs) and its main copolymers: synthesis, blends, composites, biodegradability, and applications. Polymers 14(4):844. https://doi.org/10.3390/polym14040844

Alves L, Ferraz E, Gamelas J (2019) Composites of nanofibrillated cellulose with clay minerals: a review. Adv Colloid Interface Sci 272(101):994. https://doi.org/10.1016/j.cis.2019.101994

An DS, Lee JH, Lee DS (2018) Water vapor and oxygen barrier estimation in designing a single-serve package of powdered infant formula for required shelf life. J Food Process Eng 41(1):e12592. https://doi.org/10.1111/jfpe.12592

Aulin C, Strö G (2013) Multilayered alkyd resin/nanocellulose coatings for use in renewable packaging solutions with a high level of moisture resistance. Ind Eng Chem Res 52(7):2582–2589. https://doi.org/10.1021/ie301785a

Aulin C, Salazar-Alvarez G, Lindström T (2012) High strength, flexible and transparent nanofibrillated cellulose-nanoclay biohybrid films with tunable oxygen and water vapor permeability. Nanoscale 4(20):6622–6628. https://doi.org/10.1039/C2NR31726E

Aulin C, Karabulut E, Tran A et al. (2013) Transparent nanocellulosic multilayer thin films on polylactic acid with tunable gas barrier properties. ACS Appl Mater Interfaces 5(15):7352–7359. https://doi.org/10.1021/am401700n

Bauer AS, Tacker M, Uysal-Unalan I et al. (2021) Recyclability and redesign challenges in multilayer flexible food packaging-a review. Foods 10(11):2702. https://doi.org/10.3390/foods10112702

Beneventi D, Chaussy D, Curtil D et al. (2014) Highly porous paper loading with microfibrillated cellulose by spray coating on wet substrates. Ind Eng Chem Res 53(27):10982–10989. https://doi.org/10.1021/ie500955x

Beneventi D, Zeno E, Chaussy D (2015) Rapid nanopaper production by spray deposition of concentrated microfibrillated cellulose slurries. Ind Crops Prod 72:200–205

Bollström R, Nyqvist R, Preston J et al. (2013) Barrier properties created by dispersion coating. Tappi J 12(4):45–51. https://doi.org/10.32964/TJ12.4.45

Cherian RM, Tharayil A, Varghese RT et al. (2022) A review on the emerging applications of nano-cellulose as advanced coatings. Carbohydr Polym 282(119):123. https://doi.org/10.1016/j.carbpol.2022.119123

Cherpinski A, Torres-Giner S, Vartiainen J et al. (2018) Improving the water resistance of nanocellulose-based films with polyhydroxyalkanoates processed by the electrospinning coating technique. Cellulose 25(2):1291–1307. https://doi.org/10.1007/s10570-018-1648-z

Chowdhury RA, Clarkson C, Youngblood J (2018) Continuous roll-to-roll fabrication of transparent cellulose nanocrystal (CNC) coatings with controlled anisotropy. Cellulose 25(3):1769–1781. https://doi.org/10.1007/s10570-018-1688-4

Commission E for Communication DG (2020) Circular economy action plan: for a cleaner and more competitive Europe. Publications Office of the European Union. https://doi.org/10.2779/05068

Dai L, Long Z, Chen J et al. (2017) Robust guar gum/cellulose nanofibrils multilayer films with good barrier properties. ACS Appl Mater Interfaces 9(6):5477–5485. https://doi.org/10.1021/acsami.6b14471

Delioglamnis I, Kouzi E, Tsagaraki E, et al. (2018) D2.4 public perception of bio-based products—societal needs and concerns. Tech. rep., BIOWAYS Deliverable D2.4

Elton N, Gate L, Hooper J (1999) Texture and orientation of kaolin in coatings. Clay Miner 34(1):89–98. https://doi.org/10.1180/000985599546109

Fernandez-Santos J, Valls C, Cusola O et al. (2021) Improving filmogenic and barrier properties of nanocellulose films by addition of biodegradable plasticizers. ACS Sustain Chem Eng 9(29):9647–9660. https://doi.org/10.1021/acssuschemeng.0c09109

Foundation EM (2021) The global commitment 2021 progress report. Tech Rep, Ellen MacArthur Foundation, https://emf.thirdlight.com/link/n1ipti7a089d-ekf911/@/preview/1?o

Future Market Insights (2021) Food packaging market outlook (2022-2032). Tech rep, Future Market Insights, Inc., https://www.futuremarketinsights.com/reports/food-packaging-market

FutureMarkets (2021) The nanocellulose market, production and pricing report 2021. Tech Rep, Future Markets Inc., https://www.futuremarketsinc.com/the-nanocellulose-market-production-and-pricing-report-2021/

Gaffey J, McMahon H, Marsh E et al. (2021) Understanding consumer perspectives of bio-based products-a comparative case study from Ireland and The Netherlands. Sustainability. https://doi.org/10.3390/su13116062

Guerin D, Rharbi Y, Huber P, et al. (2020) Process and device for manufacturing a laminated material comprising a fibrillated cellulose layer. US Patent no. US10618015B2, date 14-April 2020

Haider TP, Völker C, Kramm J et al. (2019) Plastics of the future? the impact of biodegradable polymers on the environment and on society. Angew Chem Int Ed 58(1):50–62. https://doi.org/10.1002/anie.201805766

Herrera MA, Mathew AP, Oksman K (2017) Barrier and mechanical properties of plasticized and cross-linked nanocellulose coatings for paper packaging applications. Cellulose 24:3969–3980. https://doi.org/10.1007/s10570-017-1405-8

Hult EL, Iotti M, Lenes M (2010) Efficient approach to high barrier packaging using microfibrillar cellulose and shellac. Cellulose 17(3):575–586. https://doi.org/10.1007/s10570-010-9408-8

Jung K, Ji Y, Jeong TJ et al. (2022) Roll-to-roll, dual-layer slot die coating of chitin and cellulose oxygen barrier films for renewable packaging. ACS Appl Mater Interfaces. https://doi.org/10.1021/acsami.2c09925

Kaiser K, Schmid M, Schlummer M (2017) Recycling of polymer-based multilayer packaging: A review. Recycling 3(1):1. https://doi.org/10.3390/recycling3010001

Koppolu R, Abitbol T, Kumar V et al. (2018) Continuous roll-to-roll coating of cellulose nanocrystals onto paperboard. Cellulose 25(10):6055–6069. https://doi.org/10.1007/s10570-018-1958-1

Koppolu R, Lahti J, Abitbol T et al. (2019) Continuous processing of nanocellulose and polylactic acid into multilayer barrier coatings. ACS Appl Mater Interfaces 11(12):11920–11927. https://doi.org/10.1021/acsami.9b00922

Koppolu R, Banvillet G, Ghimire H et al. (2022) Enzymatically pretreated high-solid-content nanocellulose for a high-throughput coating process. ACS Appl Nano Mater 5(8):11302–11313. https://doi.org/10.1021/acsanm.2c02423

Kumar V, Elfving A, Koivula H et al. (2016) Roll-to-roll processed cellulose nanofiber coatings. Ind Eng Chem Res 55(12):3603–3613. https://doi.org/10.1021/acs.iecr.6b00417

Lin SY, Krochta J (2003) Plasticizer effect on grease barrier and color properties of whey-protein coatings on paperboard. J Food Sci 68(1):229–233. https://doi.org/10.1111/j.1365-2621.2003.tb

Lindström T, Österberg F (2020) Evolution of biobased and nanotechnology packaging-a review. Nord Pulp Paper Res J 35(4):491–515. https://doi.org/10.1515/npprj-2020-0042

Martinez-Hermosilla GA, Mesic B, Bronlund JE (2015) A review of thermoplastic composites vapour permeability models: applicability for barrier dispersion coatings. Packag Technol Sci 28(7):565–578. https://doi.org/10.1002/pts.2125

Miettinen P, Auvinen S, Kuusipalo J, et al. (2015) Validity of traditional barrier-testing methods to predict the achievable benefits of the new generation water based barrier coatings for packaging materials. In: PTS Coating Symposium, pp 328–342

Morris BA (2017a) 1 - introduction. In: Morris BA (ed) The science and technology of flexible packaging. Plastics design library, William Andrew Publishing, Oxford, pp 3–21, https://doi.org/10.1016/B978-0-323-24273-8.

00001-0, https://www.sciencedirect.com/science/article/pii/B9780323242738000010
Morris BA (2017b) 4 - commonly used resins and substrates in flexible packaging. In: Morris BA (ed) The science and technology of flexible packaging. plastics design library, William Andrew Publishing, Oxford, pp 69–119, https://doi.org/10.1016/B978-0-323-24273-8.00004-6, https://www.sciencedirect.com/science/article/pii/B9780323242738000046
Naderi A, Lindström T, Sundström J et al. (2015) Microfluidized carboxymethyl cellulose modified pulp: a nanofibrillated cellulose system with some attractive properties. Cellulose 22(2):1159–1173. https://doi.org/10.1007/s10570-015-0577-3
Ragaert K, Delva L, Van Geem K (2017) Mechanical and chemical recycling of solid plastic waste. Waste manage 69:24–58. https://doi.org/10.1016/j.wasman.2017.07.044
Rudnik E (2013) 11 - biodegradability testing of compostable polymer materials. In: Ebnesajjad S (ed) Handbook of biopolymers and biodegradable plastics. Plastics Design Library, William Andrew Publishing, Boston, pp 213–263, https://doi.org/10.1016/B978-1-4557-2834-3.00011-2, https://www.sciencedirect.com/science/article/pii/B9781455728343000112
Satam CC, Irvin CW, Lang AW et al. (2018) Spray-coated multilayer cellulose nanocrystal-chitin nanofiber films for barrier applications. ACS Sustain Chem Eng 6(8):10637–10644. https://doi.org/10.1021/acssuschemeng.8b01536
Shanmugam K (2022) Spray coated cellulose nanofiber laminates on the paper to enhance its barrier and mechanical properties. J Sustain Environ Manag 1(1):10–17. https://doi.org/10.5281/zenodo.6206013
Siegenthaler KO, Künkel A, Skupin G et al. (2011) Ecoflex® and ecovio®: biodegradable, performance-enabling plastics. In: Rieger B, Künkel A, Coates GW et al. (eds) Synthetic biodegradable polymers. Springer, Berlin Heidelberg, pp 91–136
Sothornvit R, Krochta JM (2005) 23 - plasticizers in edible films and coatings. In: Han JH (ed) Innovations in food packaging. Food Science and Technology, Academic Press, London, pp 403–433, https://doi.org/10.1016/B978-012311632-1/50055-3, https://www.sciencedirect.com/science/article/pii/B9780123116321500553
Spence KL, Venditti RA, Rojas OJ et al. (2011) A comparative study of energy consumption and physical properties of microfibrillated cellulose produced by different processing methods. Cellulose 18(4):1097–1111. https://doi.org/10.1007/s10570-011-9533-z
Stark N, Matuana L (2021) Trends in sustainable biobased packaging materials: a mini review. Mater Today Sustain 15(100):084. https://doi.org/10.1016/j.mtsust.2021.100084
Sun Q, Schork FJ, Deng Y (2007) Water-based polymer/clay nanocomposite suspension for improving water and moisture barrier in coating. Compos Sci Technol 67(9):1823–1829. https://doi.org/10.1016/j.compscitech.2006.10.022
Thomas B, Raj MC, Joy J et al. (2018) Nanocellulose, a versatile green platform: from biosources to materials and their applications. Chem Rev 118(24):11575–11625. https://doi.org/10.1021/acs.chemrev.7b00627
Torres-Giner S, Figueroa-Lopez KJ, Melendez-Rodriguez B, et al. (2021) Emerging trends in biopolymers for food packaging. In: Athanassiou A (ed) Sustainable food packaging technology. John Wiley & Sons, Ltd, pp 1–33, https://doi.org/10.1002/9783527820078.ch1
Tyagi P, Salem KS, Hubbe MA et al. (2021) Advances in barrier coatings and film technologies for achieving sustainable packaging of food products-a review. Trends Food Sci Technol 115:461–485. https://doi.org/10.1016/j.tifs.2021.06.036
Vartiainen J, Shen Y, Kaljunen T et al. (2016) Bio-based multilayer barrier films by extrusion, dispersion coating and atomic layer deposition. J Appl Polym Sci. https://doi.org/10.1002/app.42260
Vieira MGA, Da Silva MA, Dos Santos LO et al. (2011) Natural-based plasticizers and biopolymer films: a review. Eur Polym J 47(3):254–263. https://doi.org/10.1016/j.eurpolymj.2010.12.011
Vilarinho F, Sanches Silva A, Vaz MF et al. (2018) Nanocellulose in green food packaging. Crit Rev Food Sci Nutr 58(9):1526–1537. https://doi.org/10.1080/10408398.2016.1270254
Wågberg L, Decher G, Norgren M et al. (2008) The build-up of polyelectrolyte multilayers of microfibrillated cellulose and cationic polyelectrolytes. Langmuir 24(3):784–795. https://doi.org/10.1021/la702481v
Wang J, Gardner DJ, Stark NM et al. (2018) Moisture and oxygen barrier properties of cellulose nanomaterial-based films. ACS Sustain Chem Eng 6(1):49–70. https://doi.org/10.1021/acssuschemeng.7b03523
Wu F, Misra M, Mohanty AK (2021) Challenges and new opportunities on barrier performance of biodegradable polymers for sustainable packaging. Prog Polym Sci 117(101):395. https://doi.org/10.1016/j.progpolymsci.2021.101395
Zhao JH, Wang XQ, Zeng J et al. (2005) Biodegradation of poly (butylene succinate) in compost. J Appl Polym Sci 97(6):2273–2278
Zhao K, Wang W, Teng A et al. (2020) Using cellulose nanofibers to reinforce polysaccharide films: blending vs layer-by-layer casting. Carbohydr Polym 227(115):264. https://doi.org/10.1016/j.carbpol.2019.115264
Zhu Y, Bousfield D, Gramlich WM (2019) The influence of pigment type and loading on water vapor barrier properties of paper coatings before and after folding. Prog Org Coat 132:201–210. https://doi.org/10.1016/j.porgcoat.2019.03.031